ELSEVIER

Journal of Fluids and Structures 25 (2009) 666–675

JOURNAL OF FLUIDS AND STRUCTURES

www.elsevier.com/locate/jfs

Low drag solutions for suppressing vortex-induced vibration of circular cylinders

G.R.S. Assi[a,*], P.W. Bearman[a], N. Kitney[b]

[a]*Department of Aeronautics, Imperial College, London SW7 2AZ, UK*
[b]*BP Exploration Operating Company Ltd., Sunbury-on-Thames TW16 7LN, UK*

Received 2 April 2008; accepted 7 November 2008

Abstract

Measurements are presented of response and drag for a flexibly mounted circular cylinder with low mass and damping. In one set of experiments it is free to respond in only the cross-flow direction and in a second it is free to respond in two degrees of freedom. It is shown how vortex-induced vibration can be practically eliminated by using free-to-rotate, two-dimensional control plates. Further it is shown that these devices achieve VIV suppression with drag reduction. The device producing the largest drag reduction was found to have a drag coefficient equal to about 60% of that for a plain, fixed cylinder over the Reynolds number range of the experiments, up to 30 000. The importance of torsional resistance of the devices is discussed and it is shown that if it is too low large oscillations of the device and cylinder will develop and if it is too high galloping is initiated.

Keywords: VIV Suppression; Drag reduction; Two-dimensional control plates; Circular cylinder

1. Introduction

Vortex-induced vibrations (VIV) are a continuing problem in many branches of engineering and can be particularly severe for the risers used in deepwater offshore oil operations. A widely used method for suppressing VIV of long slender bodies of circular cross section is the attachment of helical strakes. Developed originally in the wind engineering field, strakes suffer from two major problems: the first being that they increase drag and the second that, for a given strake height, their effectiveness reduces with decreases in the response parameter $m^*\zeta$, where m^* is the ratio of structural mass to the mass of displaced fluid and ζ is the structural damping expressed as a fraction of critical damping. Whereas a strake height of 10% of cylinder diameter is usually sufficient to suppress VIV in air at least double this amount is often required in water, and this increase in height is accompanied by a corresponding further increase in drag. For a fixed cylinder it is known that if regular vortex shedding is eliminated, say by the use of a long splitter plate, then drag is reduced. Hence in theory an effective VIV suppression device should be able to reduce drag rather than increase it. This idea underlies the work presented in this paper.

According to Bearman (1984) a simple analysis for a linear oscillator model of VIV assuming harmonic forcing and harmonic response shows that response is inversely proportional to the product of m^* and ζ. Hence the most rigorous

*Corresponding author.
E-mail address: g.assi05@imperial.ac.uk (G.R.S. Assi).

0889-9746/$ - see front matter © 2009 Elsevier Ltd. All rights reserved.
doi:10.1016/j.jfluidstructs.2008.11.002

way to test the effectiveness of a VIV suppression device is to work at low mass and damping. In the experiments to be described in this paper the parameter $m^*\zeta$ was equal to or less than 0.014. Owen et al. (2001) describe a method for low drag VIV suppression that had shown itself to be effective down to values of $m^*\zeta$ of about 0.5. This is the attachment of large scale bumps to induce three-dimensional separation and eliminate vortex shedding. However, later experiments at lower values of $m^*\zeta$ have shown a return of VIV with amplitudes similar to those of a plain cylinder. This behaviour has been observed by the authors with even grosser forms of continuous surface, three dimensionality where regular vortex shedding has been eliminated from the body when it is fixed but it returns when the cylinder is free to respond under conditions of low mass and damping. From this experience it is concluded that sharp-edged separation from strakes, with its accompanying high drag, is required to maintain three-dimensional separation and suppress VIV. Hence at values of $m^*\zeta$ typical for risers (less than 0.1) it seems that three-dimensional solutions are unlikely to provide the required combination of VIV suppression and low drag.

There are a number of two-dimensional control devices to weaken vortex shedding and reduce drag, with the most well known being the splitter plate. In this paper we describe the results of experiments to suppress VIV and reduce drag using various configurations of two-dimensional control devices.

2. Experimental arrangement

2.1. Flow facility

The investigation was carried out in a recirculating water channel with a free surface and a test section 0.6 m wide, 0.7 m deep and 8.4 m long. The flow speed, U, is continuously variable and flow with turbulence intensity less than 3% can be obtained up to at least 0.6 m/s. The circular cylinder model was constructed from 50 mm diameter perspex tube, giving a maximum Reynolds number of approximately 30 000, based on cylinder diameter D. With a wet-length of 650 mm (total length below water level) the resulting aspect ratio of the model was 13. Various VIV suppression devices were attached to the model and in the first set of experiments the cylinder was free to respond in only the transverse direction. In the second set it was free to respond in both the transverse and in-line directions. In order to have a reference to assess suppression effectiveness, experiments were also carried out on the cylinder without any devices, referred to here as the plain cylinder.

2.2. One-degree-of-freedom rig

Models were mounted on two different rigs: the first was a one-degree-of-freedom (1-dof) elastic system that allowed the cylinder to oscillate only in the transverse direction (Fig. 1(a)). Models were mounted on a very low damping, air bearing support system spanning the width of the test section. The cylinder was mounted such that there was a 2 mm gap between the lower end of the cylinder and the glass floor of the test section. A pair of springs connecting the moving base to the fixed supports provided the restoration force of the system, setting the natural frequency of oscillation in air (f_{y0}). An optical positioning sensor was installed to measure the y-displacement of the cylinder without introducing extra friction to damp the oscillations. Thus, the cylinder is free to oscillate only in the y-direction with a very low structural damping $\zeta = 0.7\%$, calculated as the percentage of the critical damping obtained from free decay oscillations performed in air.

2.3. Two-degree-of-freedom rig

The second rig, a two-degree-of-freedom (2-dof) system, allowed the cylinder to freely respond in both transverse and in-line directions (Fig. 1(b)). The cylinder model was mounted at the lower end of a long carbon fibre tube which formed the arm of a rigid pendulum. The top end of the arm was connected to a universal joint fixed at the ceiling of the laboratory so that the cylinder model was free to oscillate in any direction in a pendulum motion. The distance between the bottom of the cylinder and the pivoting point of the universal joint was 2800 mm. Two independent optical sensors were employed to measure displacements in the x- and y-directions. All displacement amplitudes presented for 2-dof measurements are for a location at the mid-length of the model. It should be noted that for a displacement equal to 1 diameter the inclination angle of the cylinder was only just over 1° from the vertical axis.

Two pairs of springs were installed in the x- and y-axes to set the natural frequencies in both directions of motion allowing different natural frequencies to be set for each direction. Although the cylinder was initially aligned in the vertical position, in flowing water the mean drag displaces the cylinder from its original location. To counteract this

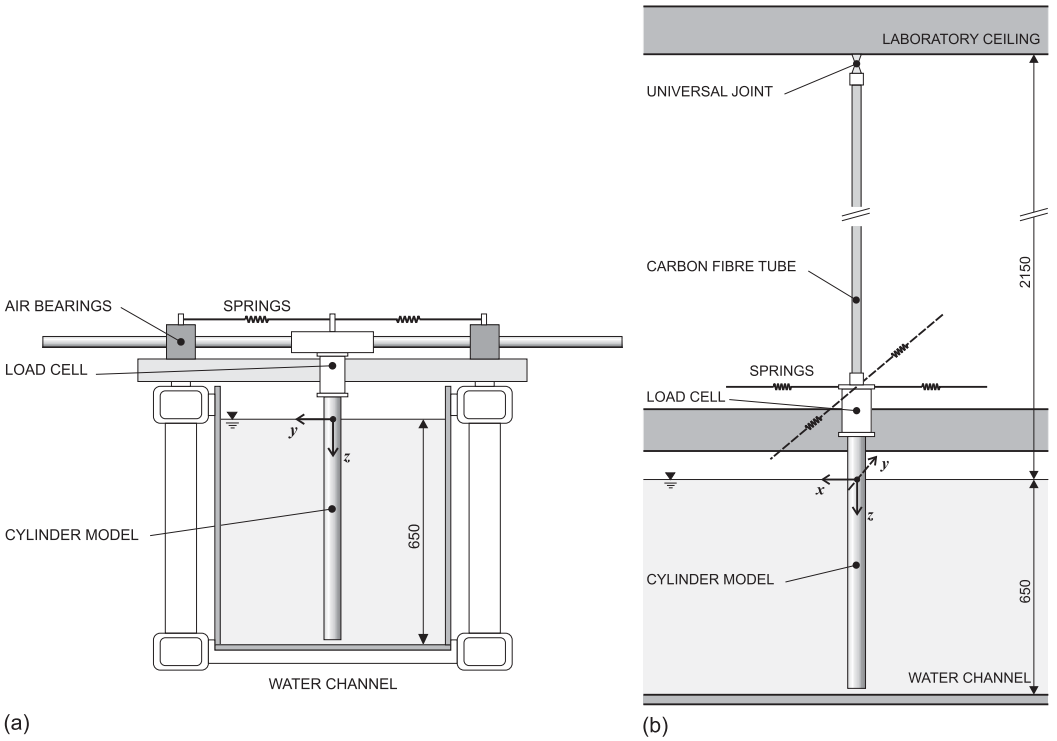

Fig. 1. Experimental apparatus: (a) 1-dof rig and (b) 2-dof rig. Water flow in x-axis.

effect, the in-line pair of springs was attached to a frame that could be moved back and forth in the direction of the flow. For each flow speed there was a position of the frame that maintained the mean position of the cylinder in the vertical direction. By using two pairs of springs perpendicular to each other, the assembly has nonlinear spring constants in the transverse and in-line directions. Movement in the transverse direction will cause a lateral spring deflection in the in-line direction and *vice versa*. This nonlinearity is minimised by making the springs as long as possible, hence the in-line springs were installed at the end of 4 m-long wires, fixed at the extremities of the frame.

It is known that during the cycle of vortex shedding from bluff bodies the fluctuation of drag has double the frequency of the fluctuation of lift. Hence a particularly severe vibration might be expected to occur if the hydrodynamic forces in both directions could be in resonance with both in-line and transverse natural frequencies at the same time. For this reason, we set the in-line natural frequency (f_{x0}) to be close to twice the transverse (f_{y0}) by adjusting the stiffness of both pairs of springs. The structural damping of the 2-dof rig was $\zeta = 0.3\%$, approximately the same for both principal directions of motion and lower than the one measured for the 1-dof rig.

In both rigs a load cell was attached between the cylinder and the support system to deduce the instantaneous and time-averaged hydrodynamic forces on the cylinder model. In order to obtain the dynamic forces acting, the inertia force (cylinder structural mass times acceleration) was subtracted from the forces recorded by the load cell. For the 1-dof tests, the mass ratio (m^*, defined as vibrating mass divided by the displaced mass of water) was adjusted by adding extra mass to the cylinder so that all models fitted with the respective devices would present the same mass ratio of 2. On the other hand, all the devices tested on the 2-dof rig were kept to the lowest possible m^* and varied between 1.6 and 2. Table 1 presents the structural parameters for all the arrangements of cylinder and suppression device tested. A description of each device presented in Fig. 2 is given later.

For each rig, measurements were made using a fixed set of springs and the reduced velocity range covered was from 1.5 to 23 for 1-dof and 1.5 to 13 for 2-dof experiments, where reduced velocity (U/Df_{y0}) is defined using the cylinder natural frequency of oscillation in the transverse direction measured in air (f_{y0}). This frequency is very close to the true natural frequency that would be recorded in a vacuum. The only flow variable changed during the course of the experiments was the flow velocity U, which, as for full-scale risers, alters both the reduced velocity and the Reynolds number.

Table 1
Structural properties and average drag coefficients with corresponding drag reduction relative to a fixed cylinder..

Model	1-dof rig		2-dof rig				
	m^*	$m^*\zeta$	m^*	$m^*\zeta$	f_{x0}/f_{y0}	$\overline{C_D}$	Drag reduction
■ Fixed cylinder	–	–	–	–	–	1.03	Reference
• Plain cylinder	2.0	0.014	1.6	0.0047	1.93	–	–
◇ Single splitter plate	2.0	0.014	1.7	0.0051	1.89	0.88	14%
○ Double splitter plates	2.0	0.014	1.8	0.0055	1.88	0.70	32%
△ Parallel plates	2.0	0.014	1.9	0.0056	1.86	0.63	38%
▷ Parallel plates with gap	2.0	0.014	2.0	0.0060	1.88	0.69	33%

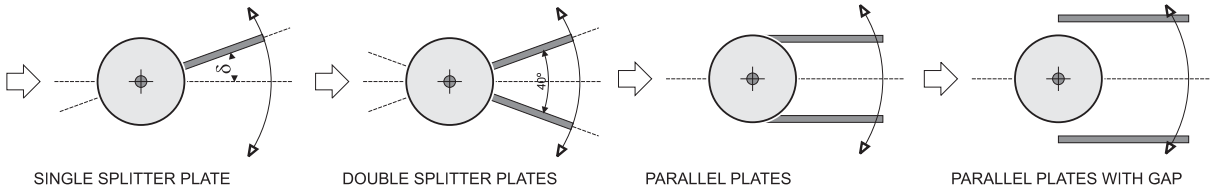

Fig. 2. Sketch of proposed control plates free to rotate abound the centre of a circular cylinder: single splitter plate (length varying from $0.25D$ to $2D$), double splitter plates, parallel plates (after Grimminger, 1945), parallel plates with $0.1D$ gap.

Throughout the study, cylinder displacement amplitudes in both directions (A_x and A_y) were found by measuring the root mean square value of response and multiplying by $\sqrt{2}$. This is likely to give an underestimation of maximum response but was judged to be perfectly acceptable for assessing the effectiveness of VIV suppression devices. Displacements A_x and A_y are nondimensionalised by dividing by the plain cylinder diameter D.

In addition to response and force measurements, flow visualisation was carried out using laser-illuminated fluorescent dye and hydrogen bubbles. Flow field measurements to obtain instantaneous spatial distributions of velocity and vorticity were obtained using a digital PIV system.

3. Experimental results and discussion

3.1. Plain cylinder results

Initially experiments were conducted on a plain cylinder to help validate the apparatus and the experimental method. Fig. 3(a) shows transverse amplitude versus reduced velocity for 1-dof and the form of the results is close to that found by other investigators. Measurements of the time mean drag coefficients versus reduced velocity for a plain responding cylinder and also a fixed cylinder are presented in Fig. 3(b).

In the same way, Figs. 7(a), (c) and (e) present transverse and in-line displacement amplitudes and drag coefficients for a plain cylinder responding in 2-dof, complemented by the trajectories of motion shown in Fig. 9. The results are repeated in other parts of Fig. 7 for comparison. These results were found to be in good agreement with those presented by other researchers.

3.2. Response of suppressors in 1-dof

3.2.1. Fixed splitter plate

Splitter plates could be rigidly attached to the rear of the cylinder and tests were carried out with plates of length (L_{SP}) between $0.25D$ and $2D$. The result in all cases was a very vigorous transverse galloping oscillation that, with increasing reduced velocity, would apparently increase without limit. In this first experiment the maximum amplitude of transverse oscillation was limited to $2D$ and this was reached at a reduced velocity of about 13 for a $1D$-long splitter plate (Fig. 3(a)). A similar galloping response was also observed for a 2-dof experiment, but these results are not presented in this paper.

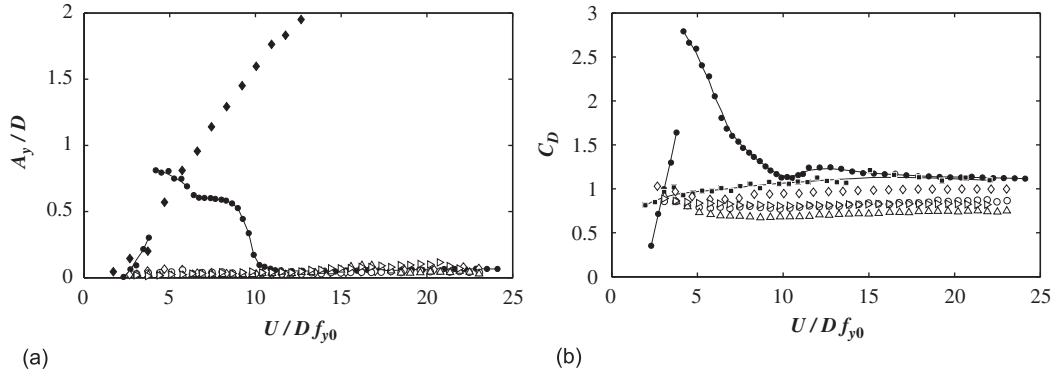

Fig. 3. Response of suppressors in 1-dof compared with a plain cylinder: (a) transverse amplitude versus reduced velocity and (b) drag coefficient versus reduced velocity. Key: •, plain oscillating cylinder; ■, plain fixed cylinder; ◆, fixed splitter plate. Free to rotate devices: ◇, single splitter plate; ○, double splitter plate; △, parallel plates; ▷, parallel plates with $0.1D$ gap.

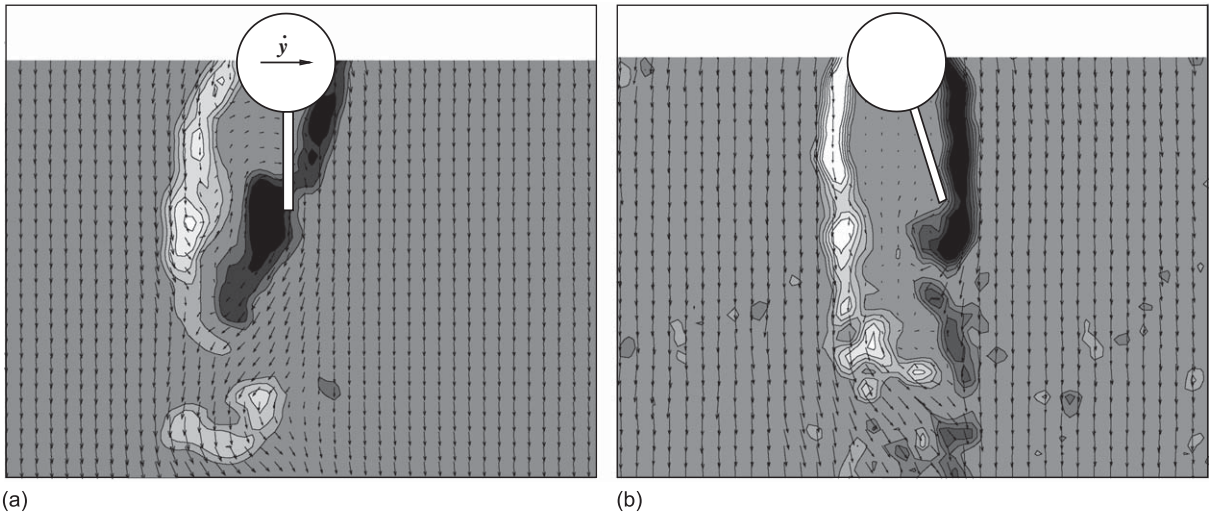

Fig. 4. Instantaneous velocity vectors and vorticity contours for fixed and f-t-r splitter plates at reduced velocity 6: (a) fixed splitter plate under galloping oscillations and (b) free-to-rotate splitter plate suppressing vibrations.

Flow visualisation and PIV measurements were carried out to investigate the interaction between the wake and the splitter plate. Fig. 4(a) presents the instantaneous velocity and vorticity fields for a reduced velocity of 6. The data was acquired when the cylinder is crossing the centreline from left to right, therefore presenting maximum transverse velocity $\dot{y}$. The vorticity contours show that the shear layer separated from the right-hand side of the cylinder apparently reattaches at the tip of the fixed splitter plate. This interaction with the tip and the proximity of the shear layer running along the splitter plate causes a region of lower pressure on the right-hand side of the plate and cylinder. A transverse force develops in the same direction as the cylinder motion, energy is extracted from the free stream and galloping oscillations are sustained in essentially the same way as for classical galloping of square section cylinders. We also note from Fig. 4(a) that the shear layers are free to interact after the splitter plate forming vortices further downstream. The behaviour described above is illustrated in Fig. 5(a) where the resultant velocity approaching the cylinder is the vectorial addition of the free stream velocity U and the cylinder's transverse velocity $\dot{y}$. Since a device to be used in the ocean must have omni-directional effectiveness the next stage was to pivot the splitter plate about the centre of the cylinder, leaving just a small gap between the plate and the cylinder surface. As with all the free-to-rotate (f-t-r) devices described, the splitter plate was mounted on bearings at each end of the cylinder.

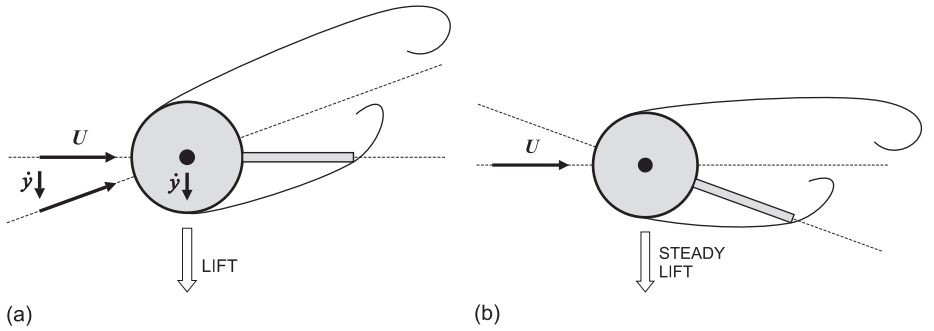

Fig. 5. Diagram showing offset position of plate and direction of steady lift force: (a) fixed splitter plate under galloping oscillations and (b) free-to-rotate splitter plate suppressing vibrations (therefore the cylinder is stationary at $\dot{y} = 0$).

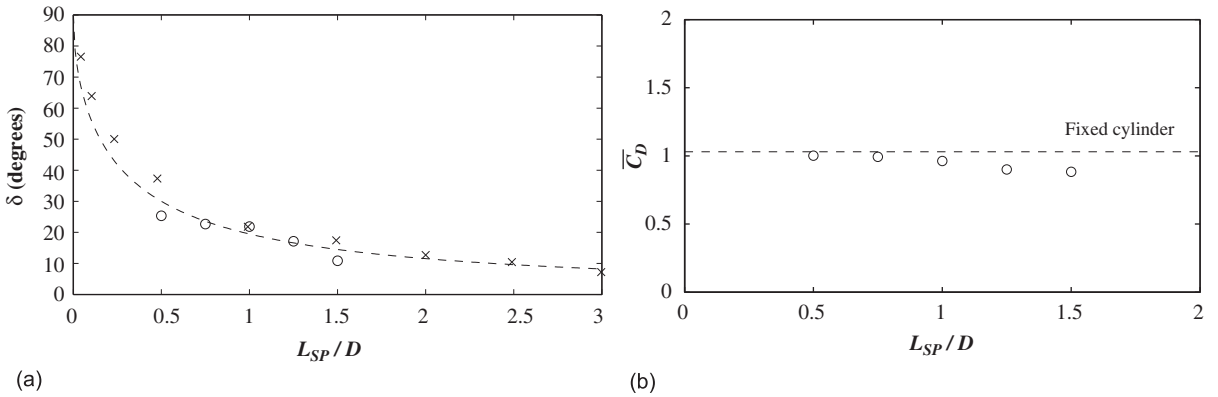

Fig. 6. Effect of splitter plate length on its offset position and cylinder drag: (a) stable offset angle versus plate length and (b) average drag coefficient versus plate length. Key: ○, present work; ×, Cimbala and Garg (1991), $5 \times 10^3 < \mathrm{Re} < 2 \times 10^4$.

3.2.2. *The free-to-rotate splitter plate*

Following the disappointing results with a fixed plate, it was hoped that a plate free to rotate might provide sufficient hydrodynamic damping to suppress the galloping. However, when an f-t-r splitter plate was used there were found to be two stable positions for the plate at roughly $\pm 20^\circ$ to the free stream direction and the plate rapidly adopted one or other of these positions when it was released. VIV was suppressed, throughout the range of reduced velocity investigated, and drag reduced below that of a plain cylinder. Cimbala and Garg (1991) also observed this bi-stable behaviour for an f-t-r cylinder fitted with a splitter plate. In their experiments the cylinder and the splitter plate were manufactured into one solid body allowed to rotate around the axis of the cylinder. However, the pivoting axis of their system was rigidly mounted on a wind tunnel section not allowing any flow-induced vibration. Our measurements of transverse response for the $1D$ f-t-r splitter plate are shown in Fig. 3(a) and time mean drag coefficients are plotted in Fig. 3(b). Results for a plain cylinder, fixed and free, are shown for comparison. The results for other devices are also shown in these figures and they will be described later.

PIV measurements presented in Fig. 4(b) show that on the side to which the plate deflected the separating shear layer from the cylinder appeared to attach to the tip of the plate and this had the effect of stabilising the near wake flow. Vortex shedding was visible downstream but this did not feed back to cause vibrations.

An unwanted effect was that a steady transverse lift force developed on the cylinder. The splitter plate was free to rotate so the force, caused by differing flow on the two sides of the combination of cylinder and splitter plate, must be acting primarily on the cylinder rather than the plate. As shown in Fig. 5(b), the direction of the force was opposite to that which occurs on an aerofoil with a deflected flap, and caused the cylinder to adopt a steady offset position to the side to which the splitter plate deflected. It was this force which was responsible for the strong galloping response with the fixed splitter plate explained earlier. As a cylinder with a fixed splitter plate aligned with the free stream plunges downwards (Fig. 5(a)), say, the instantaneous flow direction is approximately the same as that shown in Fig. 5(b).

All the results presented so far have been for an f-t-r plate having a length equal to the cylinder diameter. Further tests were carried out with a series of f-t-r splitter plates with various lengths (L_{SP}) in order to assess the effect of plate length on VIV suppression effectiveness. The results showed that f-t-r splitter plates with lengths between 0.5 and 1.5 of a cylinder diameter are all effective in suppressing VIV. Also they all had drag coefficients below the value for a plain fixed circular cylinder. When f-t-r plates outside the range $0.5D$ to $1.5D$ were attached to the cylinder a transverse flow-induced vibration returned. Cimbala and Garg (1991) found stable positions outside this range but this may have been because their system was not allowed to respond to flow-induced excitation. A secondary effect might have been the level of friction in their ball bearings (as discussed later in this paper).

The plates that successfully suppressed VIV adopted slightly different offset angles (δ, defined in Fig. 2), depending on plate length. These steady angles are plotted in Fig. 6(a) along with results from Cimbala and Garg (1991). It can be seen that the longer the splitter plate the smaller the angle. The dashed line in the figure is the angle the plate would adopt if it is assumed that the tip of the plate just intercepts a line leaving the shoulder of the cylinder and trailing back in the flow direction. The data generally support the observation that the shear layer from the side of the cylinder to which the splitter plate deflects just reattaches at its tip. Also shown in Fig. 6(b) is the variation of drag coefficient with splitter plate length. These results suggest that a successful VIV suppression and drag reduction device using a f-t-r splitter plate can be shorter than one cylinder diameter.

3.2.3. Pairs of plates

In order to try to eliminate the steady transverse force found for an f-t-r splitter plate, a pair of plates was introduced. The plates were $1D$ long and set at $\pm 20^\circ$ to the free stream direction. The angle between the plates was fixed but the pair of plates was free to pivot about the centre of the cylinder. The configuration is shown as *double splitter plates* in Fig. 2.

As shown by the results plotted in Fig. 3, this configuration suppressed VIV and reduced drag below that of a plain cylinder. It also eliminated the steady side force found with the single plate. With this arrangement the shear layers from the cylinder stabilised and reattached to the tips of the plates. Downstream of the plates vortex shedding was observed but this did not generate an excitation sufficient to cause any serious VIV. Maximum amplitudes recorded were around 5% of the cylinder diameter.

Further variations on the concept of double plates, some inspired by the early work of Grimminger (1945) related to suppressing VIV of submarine periscopes, were also studied. These included plates parallel to the flow and trailing back from the $\pm 90^\circ$ points on the cylinder. In one case there was a very small gap between the plates and the cylinder (*parallel plates* in Fig. 2) and in a second case the gap was set at 10% of the cylinder diameter (*parallel plates with gap* in Fig. 2). The plates trailed back $1D$ from the back of the cylinder. In Grimminger's experiments the plates were fixed since the flow direction was known but in our work the plates were free to rotate. It was found that the plates with the very small gap give the better performance. As shown in the plots in Fig. 3 of amplitude and drag coefficient against reduced velocity, this configuration of plates provided excellent VIV suppression and a reduction in drag below the plain cylinder value.

3.3. Response of suppressors in 2-dofs

It has been shown here that various arrangements of two-dimensional control plates are effective in suppressing transverse VIV. However, is this achieved at the expense of larger in-line VIV amplitudes? To answer this question a set of experiments was conducted in the 2-dof rig. Experiments were repeated with the various arrangements of plates and the measured transverse (A_y) and in-line (A_x) amplitudes and drag coefficients (C_D) are shown in Fig. 7 plotted against reduced velocity. Results for the plain cylinder are also shown as well as a sample of the trajectories of motion (Fig. 9) and these agree with those found by other investigators.

After confirming that all the devices would successfully suppress VIV in 1-dof oscillations, we mounted the same models in the 2-dof rig. This produced further unexpected findings. Starting with the single splitter plate, we found out that the plate was not able to stabilise in the expected $\pm 20^\circ$ position, but oscillated severely from one side to the other and the cylinder developed high amplitudes, both in-line and transverse. We observed that the splitter plate oscillated so much that it almost reached the $\pm 90^\circ$ positions. This behaviour was also observed for all the other devices. Figs. 7(a) and (c) present the transverse and in-line amplitudes versus reduced velocity and show that all devices led to considerable vibrations of the cylinder, in many cases greater than that for the plain cylinder. As one might expect, almost all drag coefficients presented in Fig. 7(e) were increased above the ones for a plain cylinder. Apart from moving from 1-dof to 2-dof, the only other change in the apparatus was to use lower friction bearings in the mounts for the suppression devices. This prompted us to consider additional parameters that might be important in stabilising the devices.

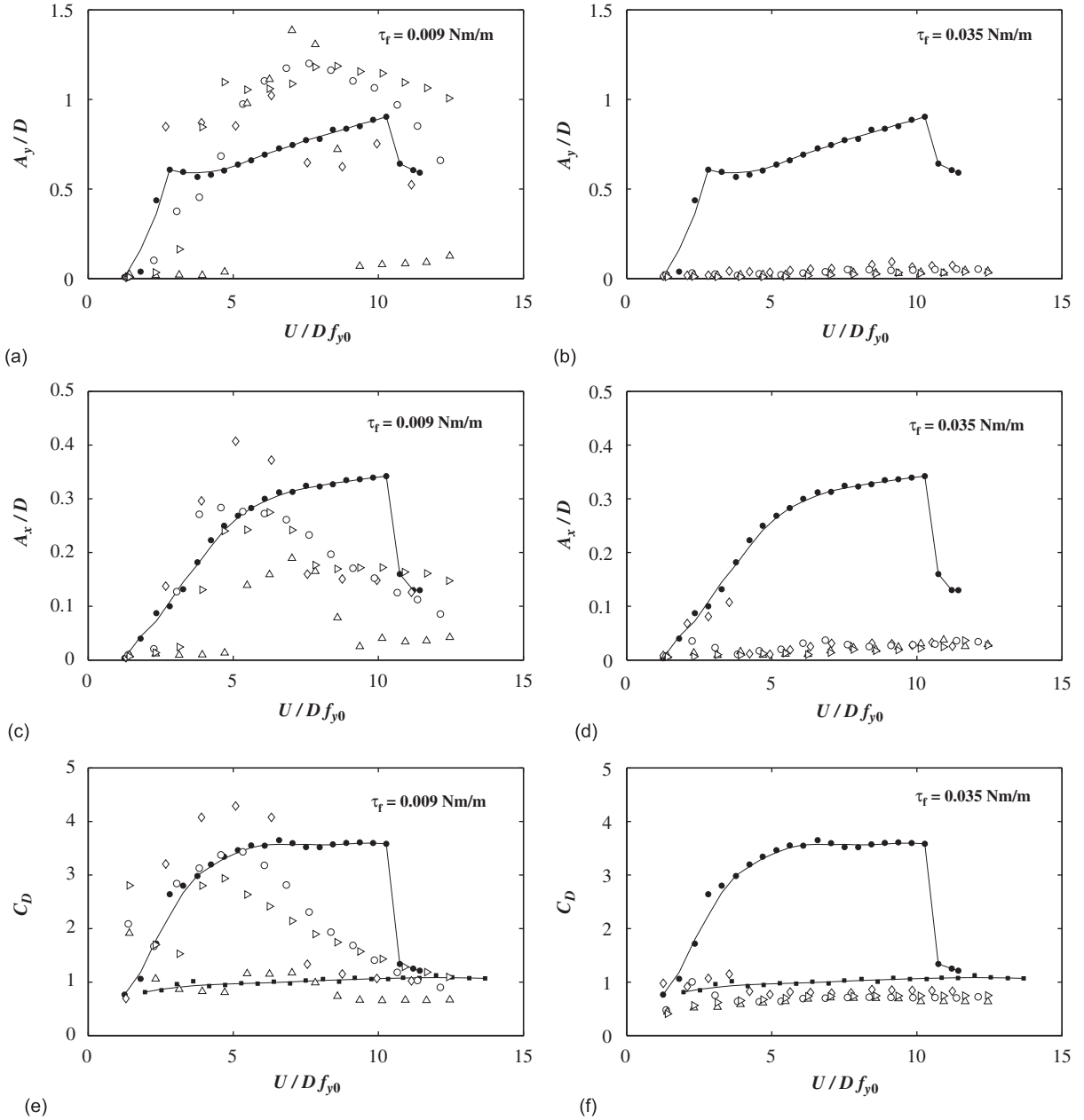

Fig. 7. Transverse displacement (top), in-line displacement (middle) and drag coefficient (bottom) versus reduced velocity for devices with 2-dof: (a), (c) and (e) torsional friction below critical value, and (b), (d) and (f) torsional friction above critical value. Key: •, plain oscillating cylinder; ■, plain fixed cylinder. Free to rotate devices: ◇, single splitter plate; ○, double splitter plate; △, parallel plates; ▷, parallel plates with $0.1D$ gap.

3.3.1. Effects of torsional resistance and rotational inertia

Two additional parameters that may influence the effectiveness of the suppression devices are: the rotational inertia of the plates and the torsional resistance resulting from friction in the bearings holding the plates. Experiments with mass added to the splitter plate to increase its rotational inertia produced no obvious change in behaviour. However, we noted that small increases in torsional friction were sufficient to suppress vibration. This finding prompted a study of

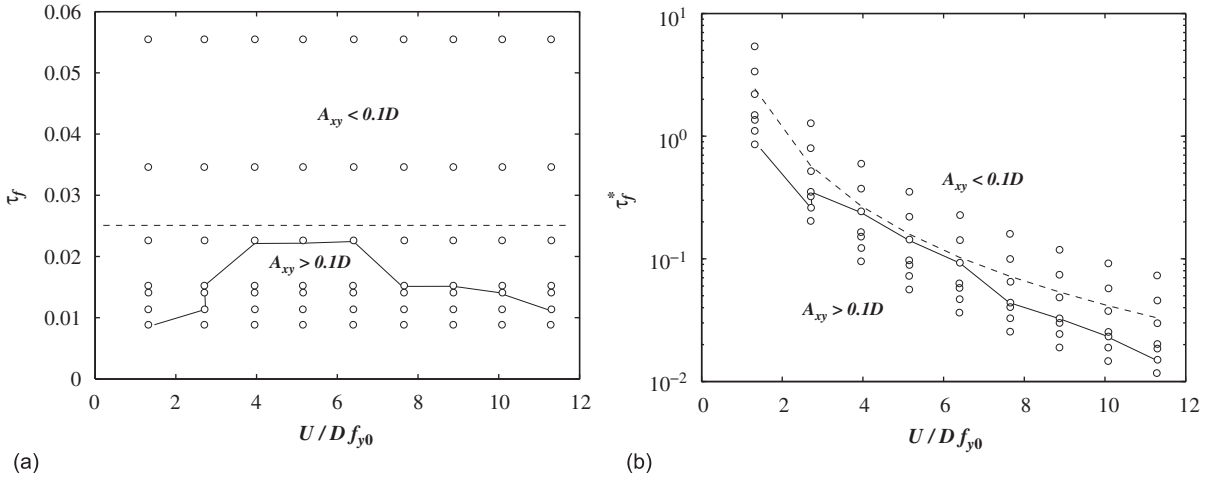

Fig. 8. VIV suppression map for an f-t-r splitter plate showing dependence on torsional friction. The solid line represents the contour where $A_{xy} = 0.1D$: (a) torsional friction versus reduced velocity and (b) nondimensionalised torsional friction parameter versus reduced velocity.

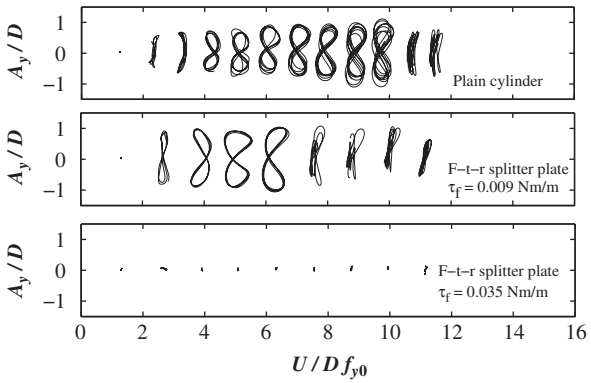

Fig. 9. A few cycles of 2-dof trajectories versus reduced velocity: plain cylinder (top), f-t-r splitter plate below critical τ_f (middle) and f-t-r splitter plate above critical τ_f (bottom). A_y/D and A_x/D are plotted to the same scale.

the effect of torsional friction which we now knew would lead to severe oscillations if it was below some critical value and presumably would result in galloping oscillations if it was too large.

A simple modification was made to the apparatus in order to control the torsional resistance (τ_f), which was varied in small increments between 0.009 and 0.055 N m per unit length of the cylinder with the lowest value being for just the bearings. With a value higher than 0.055 N m/m the splitter plate did not move over the range of reduced velocity tested and galloping returned. A nondimensional friction torque parameter is defined as $\tau_f^* = \tau_f/\rho U^2 D^2$, which represents the ratio of structural torsional resistance to a hydrodynamic torque. Use of this parameter provides a means of determining the required torsional resistance for full-scale risers.

A set of 56 runs varying the reduced velocity was completed for the single splitter plate model of length $1D$ in order to map the amplitude response for different values of τ_f. The displacement amplitude parameter A_{xy} (defined as $A_{xy} = \sqrt{A_x^2 + A_y^2}$) was determined for each run and maps of the cases studied are shown in Fig. 8. The solid line gives an indication of the effectiveness of suppression. For all points above the solid line A_{xy} is less than $0.1D$. Fig. 8(b) presents the same stability map as shown in Fig. 8(a) but instead plots the nondimensional friction torque parameter τ_f^* on the vertical axis. The dashed line is for $\tau_f = 0.025$ N m/m, illustrating that any value of torsional friction between this line and the upper threshold would be sufficient to suppress VIV with a single splitter plate.

Fig. 9 shows examples of trajectories of motion for a single splitter plate with two different torsional friction levels, below and above the critical value, compared with the response of a plain cylinder. In the low-friction case ($\tau_f = 0.009\,\mathrm{N\,m/m}$) the splitter plate was unstable and the trajectories show amplitudes higher than those for a plain cylinder. However, when the friction level was set to $0.035\,\mathrm{N\,m/m}$ the trajectories are little more than small dots over the whole range of reduced velocity.

We next wanted to verify that the other suppressors would also work if the torsional friction was set to a suitable critical value. Because the critical value was unknown for each device, we arbitrarily chose the value $\tau_f = 0.035\,\mathrm{N\,m/m}$ from the single splitter plate map of Fig. 8(a), which is in a region where suppression is effective. All devices were set at this torsional friction level and runs over a range of reduced velocity were performed. Figs. 7(b) and (d) show results that should be compared with the low-friction case ($\tau_f = 0.009\,\mathrm{N\,m/m}$). Immediately we notice that the amplitude levels in both directions of motion are very much less than those for the low-friction case. In fact, at this torsional friction level all suppressors were effective in reducing VIV below 5% of cylinder diameter. Fig. 7(f) shows that all devices reduced drag below that of a fixed cylinder for most of the range of reduced velocity and Table 1 shows that parallel plates achieved the highest average drag reduction of 38% when compared with a plain fixed cylinder. The drag coefficient data given in Table 1 for the plain cylinder and the cylinder fitted with suppression devices is an average over the range of flow velocity used (that is one value of C_D averaged between $3 \times 10^3 < Re < 3 \times 10^4$). Hence for each test case the Reynolds number range is the same and for the freely mounted models the reduced velocity ranges are also the same.

It seems likely that different suppressors might have different stability boundaries for torsional resistance, but there is clearly a range of τ_f within which VIV suppression would be achieved for the devices we studied. A further observation is that the critical torsional friction required to stabilise the splitter plate in 2-dof motion is greater than that required for 1-dof, presumably because in-line vibrations play some role.

4. Conclusions

Suppression of cross-flow and in-line VIV of a circular cylinder, with resulting drag coefficients less than that for a fixed plain cylinder, has been achieved using two-dimensional control plates. This has been accomplished at values of the combined mass and damping parameter up to 0.014. The maximum drag reduction occurs with parallel plates and is about 38%. A free-to-rotate splitter plate was also found to suppress VIV but this configuration develops a mean transverse force. This force can be eliminated by using a pair of splitter plates arranged so that the shear layers that spring from the cylinder attach to the tips of the plates.

The level of torsional friction plays a fundamentally important role, needing to be high enough to hold the devices in a stable position, while still allowing them to realign if the flow direction changes. Devices with torsional friction below a critical value oscillate themselves as the cylinder vibrates, sometimes increasing the amplitude of cylinder oscillation higher than that for a plain cylinder. All devices with torsional friction above the critical value appeared to suppress VIV and reduce drag for 1-dof and 2-dof motions. However, if the torsional resistance is above a limiting threshold the suppressors may not rotate and an undesired galloping response can be initiated.

With two-dimensional control plates proving to be effective VIV suppressors, future studies need to concentrate on optimising the devices in respect of overall length and geometry. Also, more detailed parametric studies on the effects of rotational inertia and torsional resistance should be carried out for each family of device.

Acknowledgements

The authors wish to thank BP Exploration for their support of this research. Gustavo R.S. Assi is in receipt of a Ph.D. scholarship from the Brazilian Ministry of Education (CAPES). Thanks are also due to the reviewers for pointing out the work of Cimbala and Garg (1991).

References

Bearman, P.W., 1984. Vortex shedding from oscillating bluff bodies. Annual Review of Fluid Mechanics 16, 195–222.

Cimbala, J.M., Garg, S., 1991. Flow in the wake of a freely rotatable cylinder with splitter plate. AIAA Journal 29, 1001–1003.

Grimminger, G., 1945. The effect of rigid guide vanes on the vibration and drag of a towed circular cylinder. David Taylor Model Basin Report 504.

Owen, J.C., Bearman, P.W., Szewczyk, A.A., 2001. Passive control of VIV with drag reduction. Journal of Fluids and Structures 15, 597–605.